International Journal of Non-Linear Mechanics 99 (2018) 229–239

Contents lists available at ScienceDirect

International Journal of Non-Linear Mechanics

journal homepage: www.elsevier.com/locate/nlm

A generalized quasi two-phase bulk mixture model for mass flow

Puskar R. Pokhrel [a,b,*], Khim B. Khattri [a], Bhadra Man Tuladhar [a], Shiva P. Pudasaini [c]

[a] School of Science, Kathmandu University, Dhulikhel, Kavre, Nepal
[b] Department of Mathematics, R. R. Campus, Tribhuvan University, Kathmandu, Nepal
[c] Department of Geophysics, Steinmann Institute, University of Bonn, Meckenheimer Allee 176, D-53115 Bonn, Germany

ARTICLE INFO

Keywords:
Mixture flow
Quasi-two-phase flow
Generalized bulk and shear viscosities
Generalized mixture velocities and pressure
Velocity and pressure drifts

ABSTRACT

We employ full dimensional two-phase mass flow equations (Pudasaini, 2012) [18] to develop a generalized quasi two-phase bulk model for a rapid flow of a debris mixture consisting of viscous fluid and solid particles down a channel. The emerging model, as a set of coupled partial differential equations, is characterized by some new mechanical and dynamical aspects of generalized bulk and shear viscosities, pressure, velocities and effective friction for the mixture where all these are evolving as functions of several dynamical variables, physical parameters, inertial and dynamical coefficients and drift factors. These coefficients and factors are uniquely constructed, contain the underlying physics of the system, and reveal strong coupling between the phases. The new model is mechanically described by an extended pressure and rate-dependent Coulomb-viscoplastic rheology of mixture. The model is expected to simulate the velocities and pressure of the bulk mixture much faster than the two-phase mass flow model. Furthermore, the introduction of the velocity and pressure drifts makes it possible to reconstruct the two-phase dynamics. This shows the application potential of the new model presented here.

1. Introduction

Geophysical mass flows such as debris flows, avalanches and landslides generally contain more than one material and often form a mixture of soil and rock particles with a significant to dominant quantity of interstitial fluid [1–6]. Debris flows as a typical example of geophysical mass flows, are effectively two-phase and gravity driven flows caused by intense rainfall or a sudden surge of water. Such surges may occur due to the breaking off of a saturated landmass or dam, or by a landslide event that impacts a lake, ocean or river causing over flow that may result in catastrophic dam collapse [7,8]. As the flood surge rushes down the slope, it may transform into a debris flow by entraining the bed material [9–12].

Debris flows, which generally occur in mountainous areas throughout the world, are extremely destructive and dangerous natural events. A debris flow differs from other types of mass flows including rock and snow avalanches because it contains solid particles and viscous fluid both of which generate fundamentally different forces that significantly influence the motion. During these events, the mixture material undergoes rapid motion and large deformations. The fast motion together with the evolving mixture density provides the debris flow with potentially huge energy and destructive power. Especially the interactions between solid and fluid forces can cause exceptionally long run out [4,12–14].

In simulations, debris flows are often treated as a single phase mass flows (e.g., [2,6,15]), mixture flows [3,16], a two-fluid flow [4], and a two-layered model [17]. With a major advance in two-phase debris flow modelling, Pudasaini [18] proposed a comprehensive theory and simulation technique. The model accounts for strong interactions between the solid and the fluid. The model includes buoyancy and other three important physical aspects of the flow: enhanced non-Newtonian viscous stress, virtual mass and the generalized drag. The depth-averaged version of this general two-phase mass flow model has been widely applied in different flow scenarios: rock-ice avalanche dynamic simulation [19], tsunami generated by debris impact on lakes and submarine sediment transport [20], and glacial lake outburst flood [21]. Furthermore, employing the general two-phase mass flow model [18] in the computational technique, r.avaflow, Mergili et al. [8] presented the simulation results for the interaction and propagation of mass flow in real mountain topographies. Using the same model and tool, Mergili et al. [10,22] studied the complex hydro-geomorphic process chains in a multi-lake outburst flood in the Santa Cruz Valley (Cordillera Blanca, Peru). These are the first ever explicit simulations for the evolution of the solid and fluid phase in subaerial and submarine two-phase debris flows. Numerical results indicate that the model can adequately describe the complex dynamics of subaerial two-phase debris

* Corresponding author at: School of Science, Kathmandu University, Dhulikhel, Kavre, Nepal.
E-mail address: prpokharel@student.ku.edu.np (P.R. Pokhrel).

https://doi.org/10.1016/j.ijnonlinmec.2017.12.003
Received 15 September 2017; Received in revised form 18 September 2017; Accepted 4 December 2017
Available online 14 December 2017
0020-7462/

flows, particle-laden flows, sediment transport, submarine debris flows and associated phenomena. These results highlight the applicability of the two-phase model to a wide range of geophysical mass flows.

Here, by reducing the general three-dimensional full two-phase model [18], we generate a generalized quasi two-phase full (non-depth averaged) two-dimensional model for rapid bulk mixture flow down a channel. To do so, we combine the solid and fluid phase mass balances, and similarly the momentum balance equations to obtain a quasi-two phase bulk mixture model. This is achieved by introducing the drift factors for fluid velocities and the fluid pressure in terms of the solid velocities and solid pressure, respectively. We constitute some structurally new concepts of dynamically evolving drift induced generalized barycentric velocities and pressure for the bulk mixture flow. Similarly, two further structures of bulk mixture viscosities, and the effective bulk and shear viscosities lead to the emergence of the representative complex mixture viscosity. The emerging model for bulk mixture flow consists of the full (non-depth averaged) two-dimensional quasi two-phase mass and momentum conservation equations for the generalized mixture velocities and pressure. The derived mass and momentum equations appear in non-conventional form due to the inertial coefficients, and the form of the mixture viscosities. This model structure results in a novel, dynamically evolving effective mixture friction coefficient, which made it possible to extend the pressure- and rate-dependent Coulomb-viscoplastic granular flow rheology [23,24] to the flow of debris mixtures. This is an important mechanical aspect of the derived mixture model.

Several important research activities have been carried in the past in the mixture theory of continuum mechanics [25–33]. They have focused on the modelling of a mixture of two fluids and fluid mixed with solid particles so that each component is considered as a single continuum. Iverson [13], Iverson and Denlinger [3] and Pudasaini et al. [5] progressed significantly in modelling effectively single-phase mixture flows taking into account the pore fluid pressure. Furthermore, Fernandez-Nieto et al. [17] presented two-layered model whereas Pitman and Le [4] proposed a two-fluid model for debris flow. However, our modelling approach first develops the mixture pressure, velocity and mixture shear and bulk viscosities to define the mixture stress tensor. The two-phase dynamics of solid and fluid can then be re-constructed from the definition of the mixture quantities and drift coefficients based on the known velocity and pressure of the mixture. This makes our model mechanically and structurally novel. On the one hand, the simulations based on the new model should be computationally substantially faster than the full two-phase simulations. On the other hand, such simulations are expected to be more accurate than the effectively single-phase models [3,5]. This highlights the application potential of the proposed model.

2. Three dimensional model for two-phase mass flow

In a two-phase model, the phases have distinct material properties. In general, the fluid phase is characterized by an isotropic stress distribution and a viscosity η_f and density ρ_f. Similarly, the solid phase is characterized by an anisotropic stress distribution, as a function of an internal frictional angle ϕ and the basal friction angle δ and the material density ρ_s [4,34]. The balance equations for the three-dimensional, two-phase debris flow are given by [18]:

$$\frac{\partial \alpha_s}{\partial t} + \nabla \cdot (\alpha_s \mathbf{u}_s) = 0, \tag{1}$$

$$\frac{\partial \alpha_f}{\partial t} + \nabla.(\alpha_f \mathbf{u}_f) = 0, \tag{2}$$

$$\frac{\partial}{\partial t}(\alpha_s \rho_s \mathbf{u}_s) + \nabla.(\alpha_s \rho_s \mathbf{u}_s \otimes \mathbf{u}_s) = \alpha_s \rho_s \mathbf{f} - \nabla.\alpha_s \mathbf{T}_s + p_s \nabla \alpha_s + \mathbf{M}_s, \tag{3}$$

$$\frac{\partial}{\partial t}(\alpha_f \rho_f \mathbf{u}_f) + \nabla.(\alpha_f \rho_f \mathbf{u}_f \otimes \mathbf{u}_f) = \alpha_f \rho_f \mathbf{f} - \alpha_f \nabla p_f + \nabla.\alpha_f \boldsymbol{\tau}_f + \mathbf{M}_f, \tag{4}$$

where (1) and (2) are the mass balances for the solid and fluid, and (3) and (4) are the momentum balances for the solid and the fluid phases, respectively, with

$$\begin{aligned}\mathbf{M}_s = & \frac{\alpha_s \alpha_f (\rho_s - \rho_f) g}{[\mathcal{U}_T\{\mathcal{P}\mathcal{F}(Re_p) + (1-\mathcal{P})\mathcal{G}(Re_p)\}]^J}(\mathbf{u}_f - \mathbf{u}_s)|\mathbf{u}_f - \mathbf{u}_s|^{J-1} \\ & + \alpha_s \rho_f C_{VM}\left[\left(\frac{\partial \mathbf{u}_f}{\partial t} + \mathbf{u}_f.\nabla \mathbf{u}_f\right) - \left(\frac{\partial \mathbf{u}_s}{\partial t} + \mathbf{u}_s.\nabla \mathbf{u}_s\right)\right] = -\mathbf{M}_f,\end{aligned} \tag{5}$$

$$\begin{aligned}\boldsymbol{\tau}_f = & \eta_f\left[\nabla \mathbf{u}_f + (\nabla \mathbf{u}_f)^T\right] \\ & - \eta_f \frac{\mathcal{A}(\alpha_f)}{\alpha_f}\left[(\nabla \alpha_s)(\mathbf{u}_f - \mathbf{u}_s) + (\mathbf{u}_f - \mathbf{u}_s)(\nabla \alpha_s)\right].\end{aligned} \tag{6}$$

In these model equations, t is time, α_s is the solid volume fraction, α_f $(= 1 - \alpha_s)$ is the fluid volume fraction. Similarly, $\mathbf{u}_s = (u_s, v_s, w_s)$ is the velocity vector for solid and $\mathbf{u}_f = (u_f, v_f, w_f)$ is that for fluid, $\otimes$ is the tensor product, $\mathbf{f}$ is the body force density; $\mathbf{T}_s$ is the solid stress tensor; p_s and p_f are solid and the fluid pressures; $\mathbf{M}_s$ and $\mathbf{M}_f$ $(= -\mathbf{M}_s)$ are interfacial momentum transfers for solid and fluid respectively. Furthermore, $\boldsymbol{\tau}_f$ denotes the extra stress for fluid. The exponent J can have the values 1 (for linear drag) and 2 (for quadratic drag). The first term of $\mathbf{M}_s$ is the drag force induced by the differences of the phase velocities, and the coefficient of drag $C_{DG} = \frac{\alpha_s \alpha_f (\rho_s - \rho_f) g}{[\mathcal{U}_T\{\mathcal{P}\mathcal{F}(Re_p) + (1-\mathcal{P})\mathcal{G}(Re_p)\}]^J}$ is modelled by a linear combination of solid-like $\mathcal{G}$ and fluid-like $\mathcal{F}$ drag contributions to flow resistance. $\mathcal{F}$ and $\mathcal{G}$ are functions of densities, volume fractions, and the particle Reynolds number Re_p given by $\mathcal{F} = (\rho_f/\rho_s)(\alpha_f/\alpha_s)^3 Re_p/180$ and $\mathcal{G} = \alpha_f^{M(Re_p)-1}$, where M is a parameter depending on Re_p [4,35]. The behaviour of drag depends on the interpolation parameter $\mathcal{P} \in [0, 1]$ which combines $\mathcal{G}$ and $\mathcal{F}$. Setting $\mathcal{P} = 0$ is more suitable when the solid particles are moving through a fluid and $\mathcal{P} = 1$ for flows of fluids through dense packing of grains [4,18]. The drag coefficient depends on the solid volume fraction, and increases with increasing values of α_s and $\mathcal{P}$. The second term of $\mathbf{M}_s$ is the virtual mass force [36–41] induced by the difference in the acceleration between phases with C_{VM} as virtual mass coefficient. With virtual mass force, the solid particles may bring more fluid mass with them. This results in loss of some inertia of solid mass that induces the kinetic energy of the fluid [18]. The first term of $\boldsymbol{\tau}_f$ is the Newtonian viscous stress with T as the transpose operator, and the second term of $\boldsymbol{\tau}_f$ is an enhanced Non-Newtonian viscous stress that depends on the solid volume-fraction gradient $\nabla \alpha_s$ (also see, [18,36,38,42]). $\mathcal{A}$ is the mobility of fluid at the particle–fluid interface. There is a strong coupling between the solid and the fluid momentum transfer both through the interfacial momentum transfer, which includes the viscous drag, the virtual mass force; and the enhanced viscous fluid stress.

3. A quasi two-phase generalized bulk mixture model

Here, by reducing the three-dimensional, full two-phase model (1)–(4), we generate a generalized quasi two-phase, full two-dimensional model for rapid bulk mixture flow down a channel. For simplicity, we assume that the difference between the phase accelerations is negligible, i.e., the virtual mass coefficient is close to zero, and the non-Newtonian term in the fluid extra stress tensor is insignificant. However, we note that in the following model formulations, these terms could be retained and the model can be extended for three-dimensional unconfined flows. Let $\mathbf{u}_s = (u_s, w_s)$, $\mathbf{u}_f = (u_f, w_f)$ be the respective velocity components for solid and fluid in the down-slope (x) and perpendicular to the channel surface (z) directions as shown in Fig. 1. Since $\alpha_s + \alpha_f = 1$, adding the mass balance equations (1) and (2), we get the mixture mass balance

$$\nabla.(\alpha_s \mathbf{u}_s + \alpha_f \mathbf{u}_f) = 0. \tag{7}$$

In order to develop a reduced, but generalized quasi two-phase bulk mixture model we introduce the solid and fluid velocity drift coefficients [12,43–46], (λ_u, λ_w) and the pressure drift coefficient λ_p, as

$$u_f = \lambda_u u_s, w_f = \lambda_w w_s;\ p_f = \lambda_p p_s. \tag{8}$$

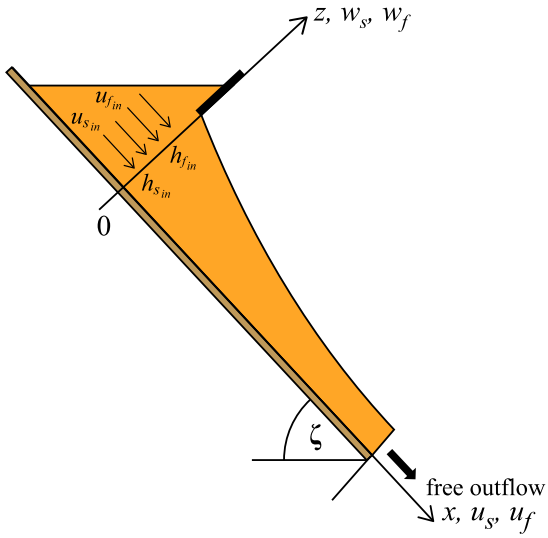

Fig. 1. Side view of the rapid flow of debris material along an inclined chute. ζ is the inclination angle, $(u_{s_{in}}, u_{f_{in}})$ and $(h_{s_{in}}, h_{f_{in}})$ are solid and fluid phase inflow velocities and heights (modified from Domnik and Pudasaini [23]).

Then (7) reduces to

$$\frac{\partial}{\partial x}\left[(\alpha_s + \lambda_u \alpha_f)u_s\right] + \frac{\partial}{\partial z}\left[(\alpha_s + \lambda_w \alpha_f)w_s\right] = 0. \tag{9}$$

This mass balance is explicitly written in terms of the solid phase (velocities). However, the fluid-phase is also represented through the velocity drift parameters (λ_u, λ_w). Interestingly, it reduces to a traditional single-phase bulk mass balance when $\lambda_u = \lambda_w = 1$, which does not distinguish between the solid and fluid velocity, or the phase dynamics [3,5,17].

As the solid and fluid phases separately are considered to be incompressible [47], ρ_s and ρ_f are both constants. Dividing by ρ_s and ρ_f on both sides of (3) and (4) respectively, we get

$$\frac{\partial}{\partial t}(\alpha_s \mathbf{u}_s) + \nabla.(\alpha_s \mathbf{u}_s \otimes \mathbf{u}_s) = \alpha_s \mathbf{f} - \frac{\alpha_s}{\rho_s}\nabla p_s + \nabla.\frac{\alpha_s}{\rho_s}\boldsymbol{\tau}_s + \frac{\mathbf{M}_s}{\rho_s}, \tag{10}$$

$$\frac{\partial}{\partial t}(\alpha_f \mathbf{u}_f) + \nabla.(\alpha_f \mathbf{u}_f \otimes \mathbf{u}_f) = \alpha_f \mathbf{f} - \frac{\alpha_f}{\rho_f}\nabla p_f + \nabla.\frac{\alpha_f}{\rho_f}\boldsymbol{\tau}_f + \frac{\mathbf{M}_f}{\rho_f}, \tag{11}$$

where, the solid and fluid Cauchy stresses are now written in terms of the solid and fluid pressures (p_s, p_f) and deviatoric stresses $(\boldsymbol{\tau}_s, \boldsymbol{\tau}_f)$, respectively [38]. Following Domnik and Pudasaini [23] and Domnik et al. [24], we will model the internal deformation of the solid component in debris bulk as a Coulomb-viscoplastic material with yield strength [48–53]. The extra fluid stress tensor $\boldsymbol{\tau}_f$ for fluid, and $\boldsymbol{\tau}_s$ for solid are [24,54–56]

$$\boldsymbol{\tau}_f = \eta_f\left[\nabla \mathbf{u}_f + (\nabla \mathbf{u}_f)^T\right], \quad \boldsymbol{\tau}_s = 2\eta_s \mathbf{D}_s + 2\tau_{y_s}\frac{\mathbf{D}_s}{\|\mathbf{D}_s\|}. \tag{12}$$

Here, $\boldsymbol{\tau}_s$ is the deviatoric stress tensor for a viscoplastic material (granular fluid). With the yield stress $\tau_{y_s} = \tau_c + \tau_p p_s$, where τ_c is cohesion, it becomes pressure- and rate-dependent Coulomb-viscoplastic law for solid-phase [23,24,57,58]. As in the fluid, the symmetric part of the velocity gradient $\mathbf{D}_s = \frac{1}{2}[\nabla \mathbf{u}_s + (\nabla \mathbf{u}_s)^T]$ is the strain-rate tensor, and η_s is the dynamic viscosity. The norm of $\mathbf{D}_s$ is defined by $\|\mathbf{D}_s\| = \sqrt{2\mathrm{tr}\,(\mathbf{D}_s^2)}$ [23,49]. The effective kinematic viscosity for solid takes the form:

$$\nu_s^e = \nu_s + \frac{\tau_{y_s}}{\|\mathbf{D}_s\|}, \tag{13}$$

where $\nu_s = \eta_s/\rho_s$ and $\tau_{y_s} := \tau_{y_s}/\rho_s$ are the solid kinematic viscosity and yield stress normalized by the solid density. During the mass flow, with $\tau_{y_s} = 0$, the material behaves as a Newtonian fluid for which $\nu_s^e = \nu_s$. Now, $\boldsymbol{\tau}_s$ in (12) can be written as $\boldsymbol{\tau}_s = 2\nu_s^e \mathbf{D}_s$, where $\boldsymbol{\tau}_s := \boldsymbol{\tau}_s/\rho_s$. In what follows, for simplicity, we replace ν_e^s by ν_s.

Next, we construct a generalized single momentum balance equation for a bulk mixture flow. Adding (10) and (11), we get:

$$\begin{aligned}&\frac{\partial}{\partial t}(\alpha_s \mathbf{u}_s + \alpha_f \mathbf{u}_f) + \nabla\cdot[(\alpha_s \mathbf{u}_s \otimes \mathbf{u}_s) + (\alpha_f \mathbf{u}_f \otimes \mathbf{u}_f)]\\ &\quad = \mathbf{f} + \nabla\cdot\left(\alpha_s \boldsymbol{\tau}_s + \alpha_f \boldsymbol{\tau}_f\right) - \left(\alpha_s \nabla p_s + \alpha_f \nabla p_f\right) + \frac{\mathbf{M}_s}{\rho_s} + \frac{\mathbf{M}_f}{\rho_f},\end{aligned} \tag{14}$$

where, pressures (p_s, p_f) and stresses $(\boldsymbol{\tau}_s, \boldsymbol{\tau}_f)$ are normalized with respective densities, and the viscosities in $(\boldsymbol{\tau}_s, \boldsymbol{\tau}_f)$ are kinematic viscosities. With $u_f = \lambda_u u_s$ and $w_f = \lambda_w w_s$, the local time derivative of the 'mixture velocity' in (14) becomes

$$\frac{\partial}{\partial t}(\alpha_s \mathbf{u}_s + \alpha_f \mathbf{u}_f) = \frac{\partial}{\partial t}\left[(\alpha_s + \lambda_u \alpha_f)u_s,\ \ (\alpha_s + \lambda_w \alpha_f)w_s\right]. \tag{15}$$

The convective terms in (14) can be written as

$$\begin{aligned}&\nabla\cdot[(\alpha_s \mathbf{u}_s \otimes \mathbf{u}_s) + (\alpha_f \mathbf{u}_f \otimes \mathbf{u}_f)]\\ &\quad = \Big(\frac{\partial}{\partial x}[(\alpha_s + \lambda_u^2 \alpha_f)u_s^2] + \frac{\partial}{\partial z}[(\alpha_s + \lambda_u \lambda_w \alpha_f)u_s w_s],\\ &\quad \frac{\partial}{\partial x}[(\alpha_s + \lambda_u \lambda_w \alpha_f)u_s w_s] + \frac{\partial}{\partial z}[(\alpha_s + \lambda_w^2 \alpha_f)w_s^2]\Big).\end{aligned} \tag{16}$$

The divergence of the rate-of-strain tensors in (14) become

$$\begin{aligned}&\nabla\cdot\left[\alpha_f \boldsymbol{\tau}_f + \alpha_s \boldsymbol{\tau}_s\right]\\ &= \Big[\frac{\partial}{\partial x}\left(2\nu_f \alpha_f \frac{\partial u_f}{\partial x}\right) + \frac{\partial}{\partial z}\left(\nu_f \alpha_f\left(\frac{\partial u_f}{\partial z} + \frac{\partial w_f}{\partial x}\right)\right)\\ &\quad + \frac{\partial}{\partial x}\left(2\nu_s \alpha_s \frac{\partial u_s}{\partial x}\right) + \frac{\partial}{\partial z}\left(\nu_s \alpha_s\left(\frac{\partial u_s}{\partial z} + \frac{\partial w_s}{\partial x}\right)\right),\\ &\quad \frac{\partial}{\partial x}\left(\nu_f \alpha_f\left(\frac{\partial u_f}{\partial z} + \frac{\partial w_f}{\partial x}\right)\right) + \frac{\partial}{\partial z}\left(2\nu_f \alpha_f \frac{\partial w_f}{\partial z}\right)\\ &\quad + \frac{\partial}{\partial x}\left(\nu_s \alpha_s\left(\frac{\partial u_s}{\partial z} + \frac{\partial w_s}{\partial x}\right)\right) + \frac{\partial}{\partial z}\left(2\nu_s \alpha_s \frac{\partial w_s}{\partial z}\right)\Big]\\ &= \Big[2\frac{\partial}{\partial x}\left((\nu_s \alpha_s + \lambda_u \nu_f \alpha_f)\frac{\partial u_s}{\partial x}\right)\\ &\quad + \frac{\partial}{\partial z}\left((\nu_s \alpha_s + \lambda_u \nu_f \alpha_f)\frac{\partial u_s}{\partial z} + (\nu_s \alpha_s + \lambda_w \nu_f \alpha_f)\frac{\partial w_s}{\partial x}\right),\\ &\quad \frac{\partial}{\partial x}\left((\nu_s \alpha_s + \lambda_u \nu_f \alpha_f)\frac{\partial u_s}{\partial z} + (\nu_s \alpha_s + \lambda_w \nu_f \alpha_f)\frac{\partial w_s}{\partial x}\right)\\ &\quad + 2\frac{\partial}{\partial z}\left((\nu_s \alpha_s + \lambda_w \nu_f \alpha_f)\frac{\partial w_s}{\partial z}\right)\Big].\end{aligned} \tag{17}$$

With the definition $p_f = \lambda_p p_s$, the bulk mixture pressure gradients in (14) become

$$-\left(\alpha_s \nabla p_s + \alpha_f \nabla p_f\right) = -\left[(\alpha_s + \lambda_p \alpha_f)\frac{\partial p_s}{\partial x},\ \ (\alpha_s + \lambda_p \alpha_f)\frac{\partial p_s}{\partial z}\right]. \tag{18}$$

For simplicity, in the above formulations, we have assumed that variations of λ_u, λ_w, λ_p with x, and z are negligible. Finally, we deal with the total interfacial momentum exchange in (14):

$$\begin{aligned}&\frac{\mathbf{M}_s}{\rho_s} + \frac{\mathbf{M}_f}{\rho_f}\\ &\quad = (1-\gamma)\frac{\alpha_s \alpha_f g}{[\mathcal{U}_T\{\mathcal{P}\mathcal{F}(Re_p) + (1-\mathcal{P})\mathcal{G}(Re_p)\}]^J}(\mathbf{u}_f - \mathbf{u}_s)|\mathbf{u}_f - \mathbf{u}_s|^{J-1}\\ &\quad - \left(\frac{1}{\gamma} - 1\right)\frac{\alpha_s \alpha_f g}{[\mathcal{U}_T\{\mathcal{P}\mathcal{F}(Re_p) + (1-\mathcal{P})\mathcal{G}(Re_p)\}]^J}(\mathbf{u}_f - \mathbf{u}_s)|\mathbf{u}_f - \mathbf{u}_s|^{J-1}.\end{aligned}$$

Since $\mathbf{u}_f - \mathbf{u}_s = \left[(\lambda_u - 1)u_s,\ (\lambda_w - 1)w_s\right]$, we have

$$\begin{aligned}\frac{\mathbf{M}_s}{\rho_s} + \frac{\mathbf{M}_f}{\rho_f} &= -\frac{1}{\gamma}(1-\gamma)^2\frac{\alpha_s \alpha_f g\left[(\lambda_u - 1)u_s,\ (\lambda_w - 1)w_s\right]}{[\mathcal{U}_T\{\mathcal{P}\mathcal{F}(Re_p) + (1-\mathcal{P})\mathcal{G}(Re_p)\}]^J}\\ &\quad \times\left|\left[(\lambda_u - 1)u_s, (\lambda_w - 1)w_s\right]\right|^{J-1},\end{aligned} \tag{19}$$

which becomes zero if $\gamma \to 1$ or $(\lambda_u \to 1,\ \lambda_w \to 1)$.

So, with $\mathbf{f} = (f_x, f_z)$ from (15)–(19), (14) yields the following x- and z- directional momentum balances for the bulk mixture:

$$\frac{\partial}{\partial t}\left[(\alpha_s + \lambda_u \alpha_f)u_s\right] + \frac{\partial}{\partial x}\left[(\alpha_s + \lambda_u^2 \alpha_f)u_s^2\right]$$

$$+\frac{\partial}{\partial z}\left[(\alpha_s+\lambda_u\lambda_w\alpha_f)u_s w_s\right]=f_x-(\alpha_s+\lambda_p\alpha_f)\frac{\partial p_s}{\partial x}$$
$$+2\frac{\partial}{\partial x}\left[(\nu_s\alpha_s+\lambda_u\nu_f\alpha_f)\frac{\partial u_s}{\partial x}\right]$$
$$+\frac{\partial}{\partial z}\left[(\nu_s\alpha_s+\lambda_u\nu_f\alpha_f)\frac{\partial u_s}{\partial z}+(\nu_s\alpha_s+\lambda_w\nu_f\alpha_f)\frac{\partial w_s}{\partial x}\right], \tag{20}$$

$$\frac{\partial}{\partial t}[(\alpha_s+\lambda_w\alpha_f)w_s]+\frac{\partial}{\partial x}[(\alpha_s+\lambda_u\lambda_w\alpha_f)u_s w_s]$$
$$+\frac{\partial}{\partial z}[(\alpha_s+\lambda_w^2\alpha_f)w_s^2)]=f_z-(\alpha_s+\lambda_p\alpha_f)\frac{\partial p_s}{\partial z}$$
$$+\frac{\partial}{\partial x}\left[(\nu_s\alpha_s+\lambda_u\nu_f\alpha_f)\frac{\partial u_s}{\partial z}+(\nu_s\alpha_s+\lambda_w\nu_f\alpha_f)\frac{\partial w_s}{\partial x}\right]$$
$$+2\frac{\partial}{\partial z}\left[(\nu_s\alpha_s+\lambda_w\nu_f\alpha_f)\frac{\partial w_s}{\partial z}\right]. \tag{21}$$

With the definition of the bulk velocities, and the pressure of the mixture flow

$$u_m=(\alpha_s+\lambda_u\alpha_f)u_s,\quad w_m=(\alpha_s+\lambda_w\alpha_f)w_s,\quad p_m=(\alpha_s+\lambda_p\alpha_f)p_s, \tag{22}$$

the inertial coefficients

$$\Lambda_{uu}=\frac{\alpha_s+\lambda_u^2\alpha_f}{(\alpha_s+\lambda_u\alpha_f)^2},\ \Lambda_{ww}=\frac{\alpha_s+\alpha_f\lambda_w^2}{(\alpha_s+\lambda_w\alpha_f)^2},$$
$$\Lambda_{uw}=\frac{\alpha_s+\lambda_u\lambda_w\alpha_f}{(\alpha_s+\lambda_u\alpha_f)(\alpha_s+\lambda_w\alpha_f)},\ \Lambda_u=\frac{1}{\alpha_s+\lambda_u\alpha_f},\ \Lambda_w=\frac{1}{\alpha_s+\lambda_w\alpha_f}, \tag{23}$$

and the dynamical coefficients for mixture viscosities and pressure

$$\Lambda_{\eta_u}=\nu_s\alpha_s+\lambda_u\nu_f\alpha_f,\ \Lambda_{\eta_w}=\nu_s\alpha_s+\lambda_w\nu_f\alpha_f,\ \Lambda_p=\alpha_s+\lambda_p\alpha_f, \tag{24}$$

from (9), (20) and (21), the new dynamical model for bulk mixture flow consists of the non depth-averaged two-dimensional quasi two-phase mass and momentum conservation equations:

$$\frac{\partial u_m}{\partial x}+\frac{\partial w_m}{\partial z}=0, \tag{25}$$
$$\frac{\partial u_m}{\partial t}+\frac{\partial}{\partial x}(\Lambda_{uu}u_m^2)+\frac{\partial}{\partial z}(\Lambda_{uw}u_m w_m)=f_x-\frac{\partial p_m}{\partial x}$$
$$+2\frac{\partial}{\partial x}\left[\Lambda_{\eta_u}\frac{\partial(\Lambda_u u_m)}{\partial x}\right]+\frac{\partial}{\partial z}\left[\Lambda_{\eta_u}\frac{\partial(\Lambda_u u_m)}{\partial z}+\Lambda_{\eta_w}\frac{\partial(\Lambda_w w_m)}{\partial x}\right], \tag{26}$$
$$\frac{\partial w_m}{\partial t}+\frac{\partial}{\partial x}(\Lambda_{uw}u_m w_m)+\frac{\partial}{\partial z}(\Lambda_{ww}w_m^2)=f_z-\frac{\partial p_m}{\partial z}$$
$$+\frac{\partial}{\partial x}\left[\Lambda_{\eta_u}\frac{\partial(\Lambda_u u_m)}{\partial z}+\Lambda_{\eta_w}\frac{\partial(\Lambda_w w_m)}{\partial x}\right]+2\frac{\partial}{\partial z}\left[\Lambda_{\eta_w}\frac{\partial(\Lambda_w w_m)}{\partial z}\right], \tag{27}$$

where, for simplicity, the relations $\Lambda_p\partial p_s/\partial x =: \partial p_m/\partial x$, and $\Lambda_p\partial p_s/\partial z =: \partial p_m/\partial z$, are defined. The simple situation being the one for which variation of Λ_p is negligible. p_m is called the "kinematic pressure" for the bulk. It appears that the dynamics of the bulk pressure, p_m is complex. We will discuss on this in more detail later. The inertial and dynamical coefficients in (26) and (27) are complex and coupled, and explicitly include the physics and dynamics of mixture, such as the solid volume fraction, solid and fluid material densities and viscosities; solid friction and yield strength, rate of deformation of solid, and velocity and pressure drift parameters. Moreover, the mass and momentum equations in (25)–(27) appear in non-conventional form due to the inertial coefficients (Λ_u, Λ_w), and the non-equality of the mixture viscosities Λ_{η_u} and Λ_{η_w}. In the form, the model equations (25)–(27) may look similar to the existing (effectively single-phase) mixture mass flow models [3,5,13]. However, there are fundamentally new aspects in the new model than those found in literature. This has been discussed in Section 5 and also in the following sections.

From the application and computational point of view, the contraction (25)–(27) is useful, because it reduces the full two-phase model to a quasi two-phase bulk model. This paves the way to apply the simple single-phase computational tools of Domnik and Pudasaini [23] and Domnik et al. [24], with some amendments to numerically solve the emerged model equations, that to a large extent, describe a mixture flow of solid particles and viscous fluid. However, at the same time, the drift parameters $(\lambda_u, \lambda_w, \lambda_p)$ contain the basic and important information relating the solid and fluid velocities, and the dynamic pressures. Further models can be developed to describe these parameters. Alternatively, laboratory or field data can be utilized either to obtain solid velocities (u_s, w_s) and pressure p_s, or fluid velocities (u_f, w_f) and pressure p_f, and simulate the dynamics for the other field variables. This makes the resulting model a generalized quasi two-phase bulk mixture model. For $\lambda_u = \lambda_w = \lambda_p = 1$ the emerging model reduces to traditional effectively single-phase bulk mixture model [3,5]. The new model has a potential for a wider application through constructing the functional relations for $(\lambda_u, \lambda_w, \lambda_p)$, or via parameterizations; the advantage is that computationally it is faster than the full two-phase simulations, and, at the same time, more accurate than the single-phase models.

4. The new model equations

Here, we present the final set of model equations that is written in a convenient form for applications and numerical simulations [24].

4.1. Pressure Poisson equations

To calculate the pressure p_m, we construct the pressure Poisson equation for the bulk mixture. The x- and z-directional momentum equations (26) and (27) can be written as

$$\frac{\partial u_m}{\partial t}=-\frac{\partial p_m}{\partial x}+F, \tag{28}$$
$$\frac{\partial w_m}{\partial t}=-\frac{\partial p_m}{\partial z}+G, \tag{29}$$

where

$$F=-\frac{\partial}{\partial x}(\Lambda_{uu}u_m^2)-\frac{\partial}{\partial z}(\Lambda_{uw}u_m w_m)+2\frac{\partial}{\partial x}\left(\Lambda_{\eta_u}\frac{\partial(\Lambda_u u_m)}{\partial x}\right)$$
$$+\frac{\partial}{\partial z}\left(\Lambda_{\eta_u}\frac{\partial(\Lambda_u u_m)}{\partial z}+\Lambda_{\eta_w}\frac{\partial(\Lambda_w w_m)}{\partial x}\right)+f_x, \tag{30}$$
$$G=-\frac{\partial}{\partial x}(\Lambda_{uw}u_m w_m)-\frac{\partial}{\partial z}(\Lambda_{ww}w_m^2)+\frac{\partial}{\partial x}\left(\Lambda_{\eta_u}\frac{\partial(\Lambda_u u_m)}{\partial z}+\Lambda_{\eta_w}\frac{\partial(\Lambda_w w_m)}{\partial x}\right)$$
$$+2\frac{\partial}{\partial z}\left(\Lambda_{\eta_w}\frac{\partial(\Lambda_w w_m)}{\partial z}\right)+f_z. \tag{31}$$

Partially differentiating (28) with respect to x, and (29) with respect to z, and adding them, we get

$$\frac{\partial}{\partial x}\left(\frac{\partial u_m}{\partial t}\right)+\frac{\partial}{\partial z}\left(\frac{\partial w_m}{\partial t}\right)=\frac{\partial}{\partial t}\left(\frac{\partial u_m}{\partial x}+\frac{\partial w_m}{\partial z}\right)$$
$$=-\frac{\partial^2 p_m}{\partial x^2}-\frac{\partial^2 p_m}{\partial z^2}+\frac{\partial F}{\partial x}+\frac{\partial G}{\partial z}.$$

This, with the continuity equation (25) results in the following pressure Poisson equation for the mixture flow

$$\frac{\partial^2 p_m}{\partial x^2}+\frac{\partial^2 p_m}{\partial z^2}=\frac{\partial F}{\partial x}+\frac{\partial G}{\partial z}. \tag{32}$$

4.2. The bulk mixture model

With the definitions of F and G from (30) and (31), the following set of x- and z-directional momentum, and pressure Poisson equation together constitute a new generalized quasi two-phase mixture mass flow model:

$$\frac{\partial u_m}{\partial t}=-\frac{\partial p_m}{\partial x}+F, \tag{33}$$
$$\frac{\partial w_m}{\partial t}=-\frac{\partial p_m}{\partial z}+G, \tag{34}$$
$$\frac{\partial^2 p_m}{\partial x^2}+\frac{\partial^2 p_m}{\partial z^2}=\frac{\partial F}{\partial x}+\frac{\partial G}{\partial z}. \tag{35}$$

The set (33)–(35) is a system of three highly non-linear partial differential equations with three unknowns, namely, the generalized mixture

velocities u_m, w_m, and pressure p_m. So, the system is closed and the numerical integration is possible provided that the coefficients

$$\Lambda_{uu} = \frac{\alpha_s + \lambda_u^2 \alpha_f}{(\alpha_s + \lambda_u \alpha_f)^2},\ \Lambda_{ww} = \frac{\alpha_s + \alpha_f \lambda_w^2}{(\alpha_s + \lambda_w \alpha_f)^2},$$
$$\Lambda_{uw} = \frac{\alpha_s + \lambda_u \lambda_w \alpha_f}{(\alpha_s + \lambda_u \alpha_f)(\alpha_s + \lambda_w \alpha_f)},\ \Lambda_u = \frac{1}{\alpha_s + \lambda_u \alpha_f},\ \Lambda_w = \frac{1}{\alpha_s + \lambda_w \alpha_f},$$

$$\Lambda_{\eta_u} = \nu_s \alpha_s + \lambda_u \nu_f \alpha_f,\ \Lambda_{\eta_w} = \nu_s \alpha_s + \lambda_w \nu_f \alpha_f,\ \Lambda_p = \alpha_s + \lambda_p \alpha_f, \tag{36}$$

are known. Eqs. (33)–(35) require appropriate boundary conditions for the velocities and pressure at the free and the basal surface, and also the initial conditions for these variables. This has been discussed in Section 8.

4.3. Modelling the drift coefficients

There are several ways to model the drift coefficients [12,43–46]. Simplified flow situations can be utilized to reduce the drift parameters λ_u and λ_w into a single one. Assuming locally small variations of α_s and λ_u, the mixture mass balance (25), and the steady state solid mass balance (1) leads to

$$w_f \approx \lambda_0 + \lambda_u w_s, \tag{37}$$

where λ_0 is an integration constant whose value can be fixed from the boundary and physical conditions. Since $w_f = \lambda_w w_s$, by replacing $\lambda_w = \lambda_0/w_s + \lambda_u$, the model equations contain effectively a single velocity drift parameter, λ_u. Note that this does not produce singularity, because while substituting λ_w in the respective terms in the model equations (33)–(36), w_s in the denominator cancels out. In particular, this shows that when $\lambda_0 \approx 0$, $\lambda_w \approx \lambda_u$. This is advantageous, because explicit descriptions are available for λ_u. Ghosh Hajra et al. [59] analytically derived an expression for λ_u, as a ratio of the fluid and solid pressure parameters β_f and β_s, $\lambda_u = \sqrt{\beta_f/\beta_s}$. Alternatively, u_s and u_f can be obtained from the fast simulations of the depth averaged equations [20,21]. Then, we may dynamically obtain $\lambda_u = u_f/u_s$. Furthermore, we may also parameterize λ_w as a function of λ_u, e.g., a linear or a quadratic relation.

5. Discussions on physical aspects of the new model

The model equations (33)–(35) are written as well structured partial differential equations in conservative form. There are several important features of the new model. Some physical aspects, implications, and applicabilities are discussed here. We have presented two new structures (concepts) of bulk mixture viscosities and pressures as functions of the solid volume fraction, solid and fluid material densities and viscosities, solid friction and yield strength, rate of deformation of solid, and velocity and pressure drift parameters. One of the advantages of the coupled and generalized model (33)–(35) is that structurally it is the same as the single phase granular or debris flow model [23,24]. So, in principle, the same computational strategy can be applied to solve the new system. However, the complexity inherited by the two-phase bulk mixture flow is contained in the parameters $\Lambda_u, \Lambda_w, \Lambda_{uu}, \Lambda_{uw}, \Lambda_{ww}, \Lambda_{\eta_u}, \Lambda_{\eta_w}, \Lambda_p$. Importantly, we can reconstruct some fundamental properties and dynamics of two-phase flows.

5.1. Reconstruction of the two-phase dynamics

The two-phase dynamics is largely lost in the classically derived effectively single-phase mixture mass flow model [3,5]. But, in our derivation, once u_m, w_m and p_m are obtained from (33)–(35), the two-phase dynamics of solid (u_s, w_s, p_s) and fluid (u_f, w_f, p_f) can be calculated from (22) and (8). That is, (u_s, w_s, p_s) are obtained from (22), and then (u_f, w_f, p_f) are systematically re-constructed from (8). However, how much reality these solutions represent depends on the physics contained in $(\lambda_u, \lambda_w, \lambda_p)$, the viscosities $(\Lambda_{\eta_u}, \Lambda_{\eta_w})$ and the description of α_s.

5.2. Effective bulk viscosity

The viscous terms appear in the momentum equations (20) and (21). From the third term on the right hand side of (20), the bulk viscosity can be obtained

$$\begin{aligned}\nu_s \alpha_s \frac{\partial u_s}{\partial x} + \nu_f \alpha_f \frac{\partial(\lambda_u u_s)}{\partial x} &= \nu_s \alpha_s \frac{\partial}{\partial x}\left[\frac{1}{\alpha_s + \lambda_u \alpha_f} u_m\right] \\ &\quad + \nu_f \alpha_f \frac{\partial}{\partial x}\left[\frac{\lambda_u}{\alpha_s + \lambda_u \alpha_f} u_m\right] \\ &\approx (\nu_s \alpha_s \Lambda_u + \nu_f \alpha_f \lambda_u \Lambda_u)\ \frac{\partial u_m}{\partial x}.\end{aligned} \tag{38}$$

Similarly, from the fourth term on the right hand side of (21), another expression for the bulk viscosity can be obtained

$$\begin{aligned}\nu_s \alpha_s \frac{\partial w_s}{\partial z} + \nu_f \alpha_f \frac{\partial(\lambda_w w_s)}{\partial z} &= \nu_s \alpha_s \frac{\partial}{\partial z}\left[\frac{1}{\alpha_s + \lambda_w \alpha_f} w_m\right] \\ &\quad + \nu_f \alpha_f \frac{\partial}{\partial z}\left[\frac{\lambda_w}{\alpha_s + \lambda_w \alpha_f} w_m\right] \\ &\approx (\nu_s \alpha_s \Lambda_w + \nu_f \alpha_f \lambda_w \Lambda_w)\ \frac{\partial w_m}{\partial z}.\end{aligned} \tag{39}$$

These expressions are valid if Λ_u and λ_u vary linearly with x, and Λ_w and λ_w vary linearly with z. These approximations separately concern the x- and z-directional bulk viscosities. The effective (representative) 'bulk viscosity' of the mixture is obtained by averaging over (38) and (39):

$$\Lambda_{\eta_m}^B := \frac{1}{2}\nu_s \alpha_s (\Lambda_u + \Lambda_w) + \frac{1}{2}\nu_f \alpha_f (\lambda_u \Lambda_u + \lambda_w \Lambda_w). \tag{40}$$

If λ_u and λ_w are increasing, then $(\Lambda_u + \Lambda_w)$ and $(\lambda_u \Lambda_u + \lambda_w \Lambda_w)$ are decreasing. Thus, the viscosity of the mixture is also decreasing. This means the higher are the fluid drifts, the faster is the fluid motion, and thus, the higher is the deformation. This results in the lower bulk viscosity, as in a shear-thinning fluid [60]. This is physically meaningful.

5.3. Effective shear viscosity

The shear viscosities are contained in the fourth term on the right hand side of (20), and similarly, the third term on the right hand side of (21):

$$\begin{aligned}&(\nu_s \alpha_s + \lambda_u \nu_f \alpha_f)\frac{\partial u_s}{\partial z} + (\nu_s \alpha_s + \lambda_w \nu_f \alpha_f)\frac{\partial w_s}{\partial x} \\ &\quad \approx (\nu_s \alpha_s + \lambda_u \nu_f \alpha_f)\Lambda_u \frac{\partial u_m}{\partial z} + (\nu_s \alpha_s + \lambda_w \nu_f \alpha_f)\Lambda_w \frac{\partial w_m}{\partial x},\end{aligned} \tag{41}$$

$$\begin{aligned}&(\nu_s \alpha_s + \lambda_u \nu_f \alpha_f)\frac{\partial u_s}{\partial z} + (\nu_s \alpha_s + \lambda_w \nu_f \alpha_f)\frac{\partial w_s}{\partial x} \\ &\quad \approx (\nu_s \alpha_s + \lambda_u \nu_f \alpha_f)\Lambda_u \frac{\partial u_m}{\partial z} + (\nu_s \alpha_s + \lambda_w \nu_f \alpha_f)\Lambda_w \frac{\partial w_m}{\partial x}.\end{aligned} \tag{42}$$

This shows that there are two contributions also for the shear viscosity. Averaging these, we obtain a representative 'shear viscosity' of the mixture:

$$\Lambda_{\eta_m}^S := \frac{1}{2}\nu_s \alpha_s \left(\Lambda_u + \Lambda_w\right) + \frac{1}{2}\nu_f \alpha_f \left(\lambda_u \Lambda_u + \lambda_w \Lambda_w\right). \tag{43}$$

So, since $\Lambda_{\eta_m}^B$ and $\Lambda_{\eta_m}^S$ are identical, (43) can be considered as the "representative mixture viscosity", Λ_{η_m}. However, these are only simplifications, and that the better representations of the viscosities are as they appear in (20), (21). In simple situations, (43) can be further reduced. If the x- and z-directional velocity drifts are identical, i.e., $\lambda_u \approx \lambda_w$ (isotropic drifts), then

$$\Lambda_{\eta_m} \approx \left(\nu_s \alpha_s + \nu_f \alpha_f \lambda_u\right)\Lambda_u = \frac{\nu_s \alpha_s + \nu_f \alpha_f \lambda_u}{\alpha_s + \lambda_u \alpha_f}. \tag{44}$$

This is a very important structure, because the mixture viscosity Λ_{η_m} can be measured in a rheometer. Fig. 2 reveals that the mixture viscosity, as represented by the simplified form (44), varies strongly with the velocity drift. The chosen parameters are $\nu_s = 4.99\ \mathrm{m^2/s}$, $\nu_f =$

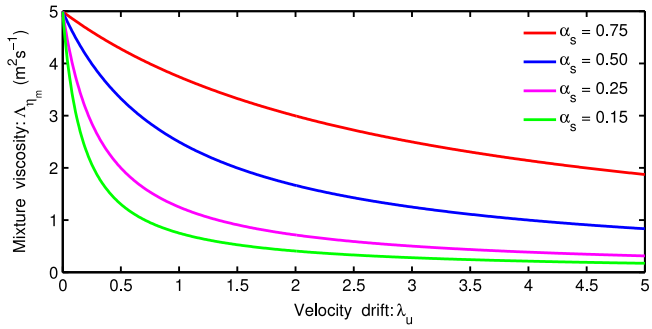

Fig. 2. Variation of the mixture viscosity with velocity drift: mixture viscosity depends strongly on the velocity drift and the solid volume fraction in the debris mixture and shows a type of shear-thinning behaviour.

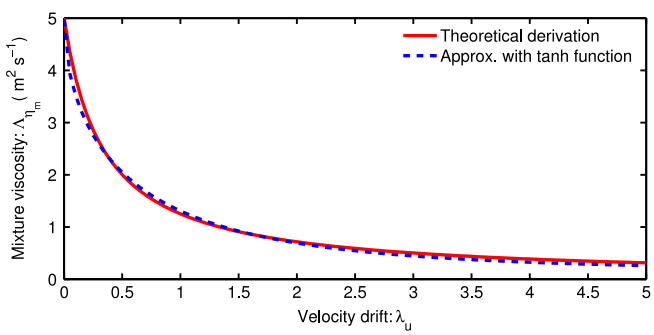

Fig. 3. Approximation of the mixture viscosity by a hyperbolic tangent function of drift.

10^{-3} m^2/s [24,57,58], and for different values of α_s. For higher solid fraction (dense flow), the drop in the mixture viscosity with the drift is slower, however, for the lower solid fraction (dilute flow), the mixture viscosity drops exponentially with the velocity drift. This indicates that the mixture flow behaves as a type of shear-thinning material: weakly for higher solid fraction but strongly with the lower solid fraction. Such a rheological behaviour of the mixture is often observed in debris flows [57,58]. Fig. 2 shows that Λ_{η_m} is an inverse exponential function of λ_u. So, it can be approximated by a hyperbolic tangent function:

$$\Lambda_{\eta_m} = \Lambda^0_{\eta_m}\left(1 - \xi \tanh(\lambda_u^{\chi})\right). \tag{45}$$

As $\Lambda^0_{\eta_m}$ is the reference value of Λ_{η_m} at $\lambda_u = 0$, this can be determined relatively easily. However ξ and χ may be determined from an experiment which is not within the scope here, but can be numerically determined for results presented in Fig. 2. Fig. 3 shows that the Λ_{η_m} in (44) can very well be represented by a hyperbolic tangent function of λ_u with the parameters $\Lambda^0_{\eta_m} = 4.99$ m^2/s, $\chi = 0.5$ and $\xi = 0.97$. This is important from an application point of view as a relatively simple function (45) can replace (44).

Furthermore, (44) shows that λ_u can be obtained analytically, and explicitly:

$$\lambda_u = \frac{(\nu_s - \Lambda_{\eta_m})\,\alpha_s}{(\Lambda_{\eta_m} - \nu_f)\,\alpha_f}. \tag{46}$$

Since usually $\nu_s - \Lambda_{\eta_m} > 0$ and $\Lambda_{\eta_m} - \nu_f > 0$, α_s, $\alpha_f > 0$, $\lambda_u > 0$. Such an explicit form of the drift is novel, and technically very important. Because, as mentioned earlier, Λ_{η_m} may be measured in the lab, then with the knowledge of ν_s and ν_f, (46) provides values for the drift, λ_u, as a function of Λ_{η_m}. This is a great advantage because this can be used to reconstruct the two-phase dynamics of the mixture. See later, Fig. 5 and Fig. 6, and the corresponding descriptions on the phase reconstructions. Fig. 4 plots (46) with $\nu_s = 4.99$ m^2/s, $\nu_f = 10^{-3}$ m^2/s, $\alpha_s = 0.25$, 0.20, 0.15, 0.10, and shows that higher is the solid volume fraction, higher

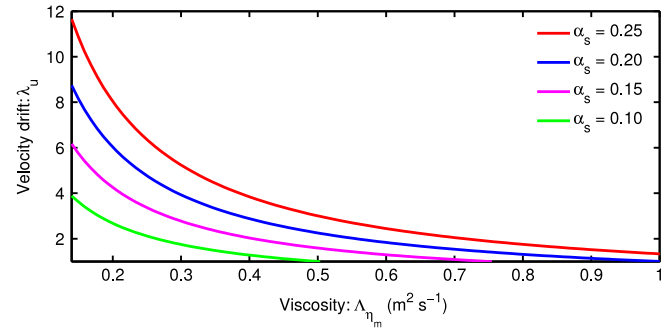

Fig. 4. Variation of the velocity drift with mixture viscosity.

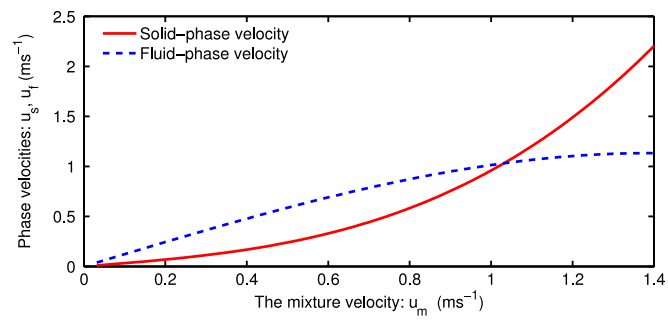

Fig. 5. Evolution of the incipient motion of mixture material that explains how the solid and fluid velocities can be reconstructed as a function of the mixture velocity.

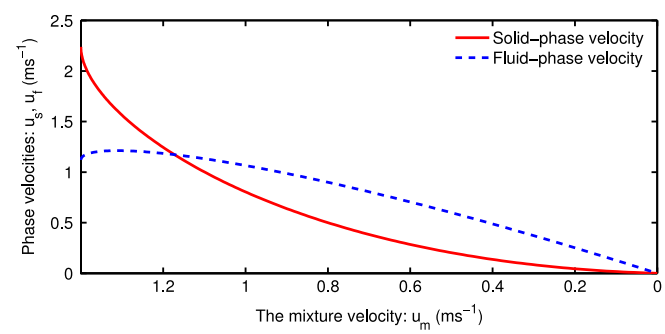

Fig. 6. Depositional behaviour of the solid and the fluid phases velocities as a function of the mixture velocity.

are the velocity drifts which decrease with higher viscosity. Fig. 2 and Fig. 4 show that the viscosity and velocity drift of the mixture flow vary inversely to each other. The same analysis can be performed for more complex mixture viscosity represented by (43).

In connection to $(22)_1$ and $(22)_2$, (46) can be utilized to reconstruct the solid and fluid velocities in terms of the mixture velocity u_m and the drift λ_u. Fig. 5 shows an incipient motion of a mixture material. The chosen parameters are $\nu_s = 4.99$ m^2/s, $\nu_f = 10^{-3}$ m^2/s, $\alpha_s = 0.25$. This figure explains how the solid and fluid velocities can be analytically reconstructed as a function of the mixture velocity. As the mass is released, the fluid accelerates faster than the solid phase, but after a while the fluid velocity tends to saturate, which is realistic [60], as the fluid-phase is a viscous material that can reach to a terminal velocity. However, the solid-phase continues to accelerate, this is also realistic because the solid phase is described by a frictional granular material. So, such an incipient behaviour can be described by our modelling approach.

Fig. 6 shows the depositional behaviour. Assume a situation, as described by Fig. 5 that after travelling a certain distance, the mixture

enters the depositional area. At the entry into the depositional area, the solid-phase has higher velocity than the fluid-phase (as seen in Fig. 5). However, as the flow enters into this area, the velocity of both the phases decrease steadily. Nevertheless, the depositional behaviour of the solid and the fluid phase are completely different. The solid decelerates much faster than the fluid. This is so, because the solid material is frictional which dissipates the energy more quickly than the fluid phase which is viscous, that is relatively weaker (because of the viscous dissipation) than the solid. These are realistic scenarios of mixture flow in depositional region.

Fig. 5 and Fig. 6 show several important features of solid and fluid velocities in the mixture flows. First, these are strongly non-linear. Second, both the solid and fluid velocities behave fundamentally differently. The rates at which the solid and fluid velocities accelerate after the mass release, and the rates of their decelerations as they enter the depositional region are completely different. These are natural phenomena, but simulated here for the first time in terms of the mixture velocity. This clearly shows the application potential of the new model presented here.

If, further, the drifts are close to unity, then

$$\Lambda_{\eta_m} \approx \nu_s \alpha_s + \nu_f \alpha_f, \tag{47}$$

which is the simplest description of the viscosity of the bulk mixture, or the concentration-weighted average viscosity [57]. The complex mixture viscosity as it appears in (40) or (43) is newly constructed here, which is rich in its physics, and evolves mechanically as a complex and coupled function of several physical and mechanical parameters and dynamical variables including the solid volume fraction α_s; solid and fluid material densities and viscosities (because the viscosities are kinematic), solid friction, yield strength and rate of deformation of solid (that appears in ν_s), and velocity and pressure (because ν_s containing yield strength that presents on solid pressure) drift parameters, etc.

5.4. Mixture pressure

The pressure of the bulk mixture is defined in (22). The solid and fluid pressures can be expressed as

$$\alpha_s \rho_s p_s = \frac{p_m \alpha_s \rho_s}{\alpha_s + \lambda_p \alpha_f}, \quad \alpha_f \rho_f p_f = \frac{(p_m \alpha_f \rho_f)\lambda_p}{\alpha_s + \lambda_p \alpha_f}. \tag{48}$$

With this, the mixture pressure can also be written as

$$p_m = \frac{\Lambda_p \left(\alpha_s \rho_s p_s + \alpha_f \rho_f p_f\right)}{\alpha_s \rho_s + \lambda_p \alpha_s \rho_f}. \tag{49}$$

In terms of generalized mixture density ($\rho_m^p = \alpha_s \rho_s + \lambda_p \alpha_f \rho_f$) with respect to pressure drift λ_p, the mixture pressure is

$$p_m = \frac{\Lambda_p}{\rho_m^p} \left(\alpha_s \rho_s p_s + \alpha_f \rho_f p_f\right).$$

This constitutes a general concept of dynamically evolving (bulk) mixture pressure. From (22) and (49), we have two equivalent representations of the mixture pressure. For dilute flows (if the extra pressure generated by the grain contacts is very small, i.e., $\lambda_p \approx 1$), then p_m reduces to

$$p_m = \frac{1}{\rho_m} \left(\alpha_s \rho_s p_s + \alpha_f \rho_f p_f\right), \tag{50}$$

where, $\rho_m = \alpha_s \rho_s + \alpha_f \rho_f$. p_m in (50) is the classical definition of the mixture (barycentric) pressure. So, (49) is called the drift induced generalized barycentric pressure for the mixture flow. This shows that λ_p may play a crucial role in the pressure dynamics. If the fluid pressure increases (say strongly, i.e., more than hydrostatic), then p_m becomes much greater than p_s. In this situation, $p_m \approx \lambda_p \alpha_f p_s$. If λ_p is very small, from (48), we obtain $p_m = \alpha_s p_s$. The pressures p_s and p_f are dynamic. So, both can be positive, or negative, or one of them positive and the other negative. Assume that $p_s > 0$, and the fluid pressure is negative ($\lambda_p < 0$). But, whether $p_m > 0$ or < 0 depends on $\alpha_s + \lambda_p \alpha_f$. If $\alpha_s + \lambda_p \alpha_f > 0$, $p_m > 0$, otherwise $p_m < 0$. So, one of the phases may have locally negative pressure, however the bulk pressure can still be positive. It may depend on, how the negative fluid pressure develops and the amount of the locally available fluid. Many other interesting possibilities can be described. For example, large shearing of the solid matrix can result in dilatation leading to the decreased fluid pressure. This implies that bulk pressure can be smaller than the solid pressure, because $\alpha_s + \lambda_p \alpha_f < 1$. On the contrary, during compaction of the solid phase, the fluid pressure increases substantially, leading to the higher bulk pressure than that of the solid. Therefore, the dynamics of the bulk pressure p_m is much more complex than just the dynamics of the solid and fluid pressures separately.

5.5. Mixture velocity

As for the bulk pressure, the bulk mixture velocities $u_m = (\alpha_s + \lambda_u \alpha_f) u_s$, $w_m = (\alpha_s + \lambda_w \alpha_f) w_s$ can be expressed as

$$u_m = \frac{\alpha_s \rho_s u_s + \alpha_f \rho_f u_f}{\Lambda_u \left(\alpha_s \rho_s + \lambda_u \alpha_f \rho_f\right)}, \quad w_m = \frac{\alpha_s \rho_s w_s + \alpha_f \rho_f w_f}{\Lambda_w \left(\alpha_s \rho_s + \lambda_w \alpha_f \rho_f\right)}.$$

With the generalized mixture densities with respect to velocity drifts λ_u and λ_w,

$$\rho_m^u = \alpha_s \rho_s + \lambda_u \alpha_f \rho_f; \quad \rho_m^w = \alpha_s \rho_s + \lambda_w \alpha_f \rho_f,$$

the mixture velocities can be written in alternative forms as

$$u_m = \frac{1}{\Lambda_u \rho_m^u} \left(\alpha_s \rho_s u_s + \alpha_f \rho_f u_f\right), \quad w_m = \frac{1}{\Lambda_w \rho_m^w} \left(\alpha_s \rho_s w_s + \alpha_f \rho_f w_f\right). \tag{51}$$

These are called the drift induced generalized barycentric velocities, or simply the generalized mixture velocities. In special situation when the velocity drifts are close to unity, these expressions reduce to the classical barycentric velocities:

$$u_m = \frac{1}{\rho_m} \left(\alpha_s \rho_s u_s + \alpha_f \rho_f u_f\right), \quad w_m = \frac{1}{\rho_m} \left(\alpha_s \rho_s w_s + \alpha_f \rho_f w_f\right). \tag{52}$$

As for the pressure, the properties of the generalized velocities can be discussed.

6. Reduced models

The models obtained in (25)–(27) can be further simplified. Here, we derive reduced models as characterized either by the volume fraction, or by the drift coefficients.

6.1. Characterization with the volume fraction

Up to now, no assumption has been made on the solid (or, fluid) volume fraction α_s. As it stands now, α_s appears to be an internal variable. There are two possibilities. (*i*) α_s can be considered as a state variable which is the general situation. This requires an extra closure or, a transport equation namely, the advection–diffusion [3,5]:

$$\frac{\partial \alpha_s}{\partial t} + u_s \frac{\partial \alpha_s}{\partial x} + w_s \frac{\partial \alpha_s}{\partial z} - D_x \frac{\partial^2 \alpha_s}{\partial^2 x} - D_z \frac{\partial^2 \alpha_s}{\partial^2 z} = 0, \tag{53}$$

which says that α_s advects with the velocity (u_s, w_s) and diffuses with (D_x, D_z). Exact solutions can be constructed in computation assuming that (u_s, w_s) and (D_x, D_z) are known for some particular time step. This can be updated as required. This way, the model equations (25)–(27) and (53) are dynamically coupled. However, much advanced sub-advection, sub-diffusion models [61] can also be utilized. (*ii*) In simple situations, either α_s can be parameterized, or be considered as constant, which is the scenario in homogeneous flow.

6.2. Characterization with drifts

6.2.1. Pressure drift factor close to unity

In situations when the solid and fluid pressure are close to each other, the pressure drift coefficient is close to unity, i.e., $\lambda_p \approx 1$.

When instantaneous pressures are in equilibrium, this can be a valid assumption, for example, if the curvature and/or the surface tension is negligible. This holds only for substantially dilute flows with very low particle contacts. When the contact area is a small fraction of the total interfacial area (e.g., loose/intermittent contacts), interfacial solid and fluid pressures can be approximated by fluid pressure [38,62]. Then, the model equations (9), (20) and (21) reduce to

$$\begin{aligned}
&\frac{\partial}{\partial x}\left[(\alpha_s+\lambda_u\alpha_f)u_s\right]+\frac{\partial}{\partial z}\left[(\alpha_s+\lambda_w\alpha_f)w_s\right]=0,\\
&\frac{\partial}{\partial t}\left[(\alpha_s+\lambda_u\alpha_f)u_s\right]+\frac{\partial}{\partial x}\left[(\alpha_s+\lambda_u^2\alpha_f)u_s^2\right]\\
&\quad+\frac{\partial}{\partial z}\left[(\alpha_s+\lambda_u\lambda_w\alpha_f)u_s w_s\right]=f_x-\frac{\partial p_s}{\partial x}\\
&\quad+2\frac{\partial}{\partial x}\left[(\nu_s\alpha_s+\lambda_u\nu_f\alpha_f)\frac{\partial u_s}{\partial x}\right]\\
&\quad+\frac{\partial}{\partial z}\left[(\nu_s\alpha_s+\lambda_u\nu_f\alpha_f)\frac{\partial u_s}{\partial z}+(\nu_s\alpha_s+\lambda_w\nu_f\alpha_f)\frac{\partial w_s}{\partial x}\right],
\end{aligned}\tag{54}$$

$$\begin{aligned}
&\frac{\partial}{\partial t}[(\alpha_s+\lambda_w\alpha_f)w_s)]+\frac{\partial}{\partial x}[(\alpha_s+\lambda_u\lambda_w\alpha_f)u_s\,w_s]\\
&\quad+\frac{\partial}{\partial z}[(\alpha_s+\lambda_w^2\alpha_f)w_s^2)]=f_z-\frac{\partial p_s}{\partial z}\\
&\quad+\frac{\partial}{\partial x}\left[(\nu_s\alpha_s+\lambda_u\nu_f\alpha_f)\frac{\partial u_s}{\partial z}+(\nu_s\alpha_s+\lambda_w\nu_f\alpha_f)\frac{\partial w_s}{\partial x}\right]\\
&\quad+2\frac{\partial}{\partial z}\left[(\nu_s\alpha_s+\lambda_w\nu_f\alpha_f)\frac{\partial w_s}{\partial z}\right].
\end{aligned}\tag{55}$$

There are only two velocity drifts remaining in these equations.

6.2.2. Identical velocity drift factors

The velocity drift factors may have the identical values in the x- and z-directions: $\lambda_u=\lambda_w\neq 1$. Then, (9), (54) and (55) reduce to

$$\frac{\partial}{\partial x}\left[(\alpha_s+\lambda_u\alpha_f)u_s\right]+\frac{\partial}{\partial z}\left[(\alpha_s+\lambda_u\alpha_f)w_s\right]=0,\tag{56}$$

$$\begin{aligned}
&\frac{\partial}{\partial t}\left[(\alpha_s+\lambda_u\alpha_f)u_s\right]+\frac{\partial}{\partial x}\left[(\alpha_s+\lambda_u^2\alpha_f)u_s^2\right]\\
&\quad+\frac{\partial}{\partial z}\left[(\alpha_s+\lambda_u^2\alpha_f)u_s w_s\right]=f_x-(\alpha_s+\lambda_p\alpha_f)\frac{\partial p_s}{\partial x}\\
&\quad+2\frac{\partial}{\partial x}\left[(\nu_s\alpha_s+\lambda_u\nu_f\alpha_f)\frac{\partial u_s}{\partial x}\right]\\
&\quad+\frac{\partial}{\partial z}\left[(\nu_s\alpha_s+\lambda_u\nu_f\alpha_f)\left(\frac{\partial u_s}{\partial z}+\frac{\partial w_s}{\partial x}\right)\right],
\end{aligned}\tag{57}$$

$$\begin{aligned}
&\frac{\partial}{\partial t}[(\alpha_s+\lambda_u\alpha_f)w_s)]+\frac{\partial}{\partial x}[(\alpha_s+\lambda_u^2\alpha_f)u_s\,w_s]\\
&\quad+\frac{\partial}{\partial z}[(\alpha_s+\lambda_u^2\alpha_f)w_s^2)]=f_z-(\alpha_s+\lambda_p\alpha_f)\frac{\partial p_s}{\partial z}\\
&\quad+\frac{\partial}{\partial x}\left[(\nu_s\alpha_s+\lambda_u\nu_f\alpha_f)\left(\frac{\partial u_s}{\partial z}+\frac{\partial w_s}{\partial x}\right)\right]\\
&\quad+2\frac{\partial}{\partial z}\left[(\nu_s\alpha_s+\lambda_u\nu_f\alpha_f)\frac{\partial w_s}{\partial z}\right].
\end{aligned}\tag{58}$$

As compared to the general situation, the advantage now is that the bulk mixture viscosity is simply given by the single expression $\nu_s\alpha_s+\lambda_u\nu_f\alpha_f$, which, however, still evolves as a function of the velocity drift λ_u, and other physical and dynamical variables included in ν_s and α_s.

6.2.3. Velocity drift factors close to unity

In the most simple situation, when the velocity drifts are close to unity ($\lambda_u,\lambda_w\approx 1$), (56)–(58) further reduce to

$$\frac{\partial u_s}{\partial x}+\frac{\partial w_s}{\partial z}=0,\tag{59}$$

$$\begin{aligned}
&\frac{\partial u_s}{\partial t}+\frac{\partial(u_s^2)}{\partial x}+\frac{\partial(u_s w_s)}{\partial z}\\
&\quad=f_x-\frac{\partial p_s}{\partial x}+2\frac{\partial}{\partial x}\left(\Lambda_m\frac{\partial u_s}{\partial x}\right)+\frac{\partial}{\partial z}\left[\Lambda_m\left(\frac{\partial u_s}{\partial z}+\frac{\partial w_s}{\partial x}\right)\right],
\end{aligned}\tag{60}$$

$$\begin{aligned}
&\frac{\partial w_s}{\partial t}+\frac{\partial(u_s\,w_s)}{\partial x}+\frac{\partial(w_s^2)}{\partial z}\\
&\quad=f_z-\frac{\partial p_s}{\partial z}+\frac{\partial}{\partial x}\left[\Lambda_m\left(\frac{\partial u_s}{\partial z}+\frac{\partial w_s}{\partial x}\right)\right]+2\frac{\partial}{\partial z}\left(\Lambda_m\frac{\partial w_s}{\partial z}\right),
\end{aligned}\tag{61}$$

where $\Lambda_m=\nu_s\alpha_s+\nu_f\alpha_f$ is now the traditional simple bulk mixture viscosity which is independent of the velocity drift. And, since the velocity drifts are close to unity, the pressure drift may also be close to unity, which is legitimate. However, for similar solid and fluid velocities, the solid and fluid pressures can be different. Even the simplest set of equations (59)–(61) is important because this includes the first order basic dynamics of evolving viscosity that governs the dynamics of the mixture flow.

7. The flow rheology

The mixture motion and the settlement are described by constitutive law. Geophysical mass flows can be modelled by viscoplastic rheology [49–51,53]. Domnik et al. [24] proposed the pressure and rate-dependent Coulomb viscoplastic rheological model to describe the full dynamics of the rapid flows of granular materials down the channels impinging on rigid walls. Unlike Herschel–Bulkley, or Bingham plasticity, Domnik et al. [24] model does not include any fit parameter, and is fully described by the phenomenological parameters of the materials. With several flow simulations, from the material collapse and silo outlet to the final depositions, they have demonstrated the applicability of their new rheological model with very high computational performances. Their model is capable of describing several important observation in wide range of geophysical mass flows as recently demonstrated by von Boetticher et al. [57,58].

Iverson [13], Iverson and Denlinger [3], Massoudi [32,33] and Pudasaini et al. [5] used the total stress in a mixture as the sum of solid and fluid-phases stress tensors. On contrary, our approach is completely different. We employ the mixture pressure, velocity and mixture shear viscosity (as constructed in Section 5, and mixture strain-rate tensor, see below), to construct the mixture stress tensor. So, flow rheology intrinsic to the model (25)–(27) is rather complex and non-conventional. It simultaneously includes the physical and dynamical properties of both the solid and fluid components. From (25)–(27), the Cauchy stress tensor for the mixture takes the form:

$$\boldsymbol{\sigma}_m=-p_m\mathbf{I}+2\Lambda_{\eta_m}\mathbf{D}_m,\tag{62}$$

where, p_m is the normalized pressure (49), Λ_{η_m} is the mixture viscosity (43)

$$\Lambda_{\eta_m}=\frac{1}{2}\nu_s^e\alpha_s\left(\Lambda_u+\Lambda_w\right)+\frac{1}{2}\nu_f\alpha_f\left(\lambda_u\Lambda_u+\lambda_w\Lambda_w\right).$$

$\mathbf{D}_m=\frac{1}{2}[\nabla\mathbf{u}_m^\Lambda+(\nabla\mathbf{u}_m^\Lambda)^T]$ is the strain-rate tensor for mixture, where $\mathbf{u}_m^\Lambda=(\Lambda_u u_m,\Lambda_w w_m)$. So, the velocity gradient terms in $\mathbf{D}_m$ are in extended and non-conventional form, and reduce to the standard form if $\Lambda_u=\Lambda_w=1$.

The effective kinematic viscosity for solid

$$\nu_s^e=\nu_s+\frac{\tau_{y_s}}{\|\mathbf{D}_m\|}\tag{63}$$

tends to infinity as $\|\mathbf{D}_m\|\to 0$. To overcome this problem in computation, Domnik et al. [24] and von Boetticher et al. [57,58] introduced the exponential factor m_y as

$$\nu_s^e=\nu_s+\frac{\tau_{y_s}}{\|\mathbf{D}_m\|}\left(1-e^{-m_y\|\mathbf{D}_m\|}\right).\tag{64}$$

To capture typical flow behaviour of a geophysical mass flow, Domnik et al. [24] proposed a pressure dependent yield stress $\tau_{y_s}=\tau_c+\tau_p p_m/\Lambda_p$, where τ_c is cohesion. Without cohesion, this forms a Drucker–Prager yield criterion [63]

$$\sqrt{\Pi_{\sigma_{D_m}}}\geqslant\tau_p p_m,\tag{65}$$

where, $\Pi_{\sigma_{D_m}}$ is the second invariant of the deviatoric stress tensor [63]. The relation (65) simply tells us that the mixture material undergoes plastic yielding when deviatoric stress is greater than the yield stress.

With several complex flow simulations, from silo outlet to the flow obstacle interactions, and depositions with solid–fluid and fluid–solid transitions, Domnik et al. [24] and von Boetticher et al. [57,58] demonstrated that the pressure-dependent yield stress discussed above is a very efficient rheological model.

8. Boundary conditions

To solve the Eqs. (25), (28)–(31) numerically, we need boundary conditions. Usually, the free surface of the debris bulk is assumed to be traction free. The friction is induced by the movement of debris mixture on the sliding plane. Consider the normal vector $\mathbf{n}$ and a tangential vector $\mathbf{t}$ on sliding plane. In rapid flows of debris material down the slopes, even the lowest particle layer in contact with the bottom boundary moves with a non-zero and non-trivial velocity. Therefore, the generally used no-slip boundary condition does not represent the flow physics [23]. A non-zero slip velocity is determined by the frictional strength, which depends on the load the material exerts on the rigid boundary. So, as in Domnik et al. [24], we relate the shear-stress $T_m^b = \boldsymbol{\sigma}_m^b \mathbf{n} \cdot \mathbf{t}$ to the normal pressure $N_m^b = \boldsymbol{\sigma}_m^b \mathbf{n} \cdot \mathbf{n}$ at the sliding surface (b). This can be achieved by using the Coulomb sliding law for bulk:

$$T_m^b = \frac{u_m^b}{|\mathbf{u}_m^b|} \tan \delta_m N_m^b, \tag{66}$$

where the tangent of the effective bed friction angle δ_m for the mixture defines the "effective proportionality constant", and $\mathbf{u}_m^b$ is the velocity of the bulk at the base. Consequently, $\delta_m \leq \delta_s$ implies the emergence of a new effective mixture friction coefficient $\mu_m = \tan \delta_m$. This is uniquely defined via (66), and reveals that μ_m or, δ_m, can evolve dynamically. Higher values of $\tan \delta_m$ go along with a higher shearing and, therefore, with a higher frictional force at the rigid boundary. The relation (66) asserts that the material yields plastically if the shear stress attains the critical value. The flowing material is assumed to be non penetrating through the boundary. So, $\mathbf{n} \cdot \mathbf{u}_m^b = 0$ and also $[(\mathbf{t} \cdot \boldsymbol{\nabla})(\mathbf{n} \cdot \mathbf{u}_m)]^b = 0$. Then, from (62), the normal and shear stresses at the bottom are given by

$$N_m^b = p_m^b + 2\Lambda_{\eta_m}^b [(\mathbf{t} \cdot \boldsymbol{\nabla})(\mathbf{t} \cdot \mathbf{u}_m)]^b, \quad \text{and} \quad T_m^b = \Lambda_{\eta_m}^b [(\mathbf{n} \cdot \boldsymbol{\nabla})(\mathbf{t} \cdot \mathbf{u}_m)]^b, \tag{67}$$

which has been expressed in terms of the tangential velocity and the pressure at the boundary, and leads to a pressure and rate-dependent Coulomb-viscoplastic sliding law. Using (67) in (66), one obtains

$$[(\mathbf{n} \cdot \boldsymbol{\nabla})(\mathbf{t} \cdot \mathbf{u}_m)]^b - 2c_m^F [(\mathbf{t} \cdot \boldsymbol{\nabla})(\mathbf{t} \cdot \mathbf{u}_m)]^b = \frac{c_m^F}{\Lambda_{\eta_m}^b} p_m^b = F_{e_m}^r p_m^b, \tag{68}$$

where the ratio between the debris friction and the viscous friction is given by $F_{e_m}^r = \frac{c_m^F}{\Lambda_{\eta_m}^b}$ (the effective friction ratio), and the friction factor c_m^F is defined by

$$c^F = \begin{cases} \dfrac{u_m^b}{|\mathbf{u}_m^b|} \tan \delta_m, & u_m^b \neq 0, \\ 0, & u_m^b = 0. \end{cases}$$

The pressure and rate-dependent Coulomb-viscoplastic sliding law for generalized bulk mixture (68), dynamically defines the bottom boundary velocity $[\mathbf{t} \cdot \mathbf{u}_m]^b$ [23]. In case, if the bed friction angle $\delta_m = 0$, then there is no solid material friction, and $c_m^F = 0$. This results in the free slip condition $[(\mathbf{n} \cdot \boldsymbol{\nabla})(\mathbf{t} \cdot \mathbf{u}_m)]^b = 0$, so the basal shear-stress vanishes. For very high shear viscosity, $F_{e_m}^r \approx 0$, and there is no more pressure dependency. So, (68) becomes

$$2c_m^F = \frac{[(\mathbf{n} \cdot \boldsymbol{\nabla})(\mathbf{t} \cdot \mathbf{u}_m)]^b}{[(\mathbf{t} \cdot \boldsymbol{\nabla})(\mathbf{t} \cdot \mathbf{u}_m)]^b}, \tag{69}$$

i.e., the friction factor is the ratio of the normal to the tangential velocity at the bottom.

We ponder the more general case, $F_{e_m}^r \neq 0$. If we consider the flow in a narrow rectangular inclined channel with the main flow direction parallel to the x-axis, the shearing mainly occurs at the bottom boundary with the basal normal vector parallel to the z-direction. The shearing at the sidewalls may not have a significant influence on the flow [24,64], and so will be neglected. Then, the Coulomb shear-stress at the bottom (66) can be written as

$$T_m^b = c_m^F \left[p_m^b + 2\Lambda_{\eta_m}^b \left(\frac{\partial u_m}{\partial x} \right)^b \right]. \tag{70}$$

So, we have extended the pressure- and rate-dependent Coulomb-viscoplastic granular flow rheology [23,24] to debris mixture flow. Moreover, the extended sliding law (68), for the rectangular inclined channel is given by

$$\left(\frac{\partial u_m}{\partial z} \right)^b - 2c_m^F \left(\frac{\partial u_m}{\partial x} \right)^b = \frac{c_m^F}{\Lambda_{\eta_m}^b} p_m^b. \tag{71}$$

The Eq. (71) is for the pressure in terms of velocity gradient or vice-versa [23]. So, the pressure dependent velocity is employed as the boundary condition at the sliding surface and the top surface is traction free. Furthermore the bottom shear stress in (71) depends only on the normal stress, i.e., on the velocity near the sliding surface.

We further employ the von Neumann boundary condition for the pressure by applying the momentum conservation in the direction of the normal at the rigid boundaries, i.e.,

$$\mathbf{n} \cdot \triangle p_m = \mathbf{n} \cdot \mathbf{F}. \tag{72}$$

This closes the derivation of the model equations and the boundary conditions for a generalized quasi two-phase mixture mass flow.

9. Essence of the new model

The full dimensional (non-depth-averaged) simulation of the debris mixture flow is a new topic. However, here, we mention some similarities and major differences between our new model and some other seemingly similar or, alternative models existing in the literature. This will make it clear the usefulness of the proposed model and its application potential.

Since, in general, all the coefficients in (36) are away from unity, even in reduced form, the convective and viscous terms in (26) and (27) are different than in Domnik and Pudasaini [23] and Domnik et al. [24]. Differences emerge from the fact that all Λ's may vary as functions of α_s's and λ's. Furthermore, (u_m, w_m) and p_m are state variables for the mixture, from which, with the knowledge of α_s and λ, the state variables for the solid $(u_s, w_s; p_s)$, and for the fluid $(u_f, w_f; p_f)$ can be reconstructed. From the technical point of view, this is a major advantage of the proposed model that could not have been achieved from classical formulations of the mixture models [3,5].

As an alternative model for the debris mixture flows, we consider von Boetticher et al. [57] in which the bulk density is computed as a linear combination of the phase densities from the knowledge of the volume fractions as transport quantities. In our formulation, we do not require to dynamically compute the bulk density. So, we do not have to deal with the difficulties with boundary conditions in simulations with the mixture density gradients and its evolutions as in von Boetticher et al. [57]. This stems from the fact that in von Boetticher et al. [57], the bulk transport equations are considered whereas we begin with two explicit mass and momentum balances for the solid and fluid phases. Then, we constructed the bulk mixture model consisting of the mass and momentum balances for the mixture. This resulted in the emergence of the velocity and pressure drift factors, inertial and dynamical coefficients for mixture velocities, viscosities and pressures. Our simple formulation provides possibilities for the construction of the full dynamics of the solid and fluid phases. This also allowed to construct several technically important reduced models that can be applied from simple to complex flow situations. The inertial, pressure and viscous terms in (33)–(35) appear in non-classical forms. Effective viscosity takes a very general form. The bulk and shear viscosities, that are in extended and general

form, are different. However, the reduced bulk and shear viscosities for the mixture appear to be equivalent. This representative mixture viscosity has further been reduced to simple mixture viscosity as in von Boetticher et al. [57] that also includes the power law rheology together with the yield strength for the slurry fluid, whereas we model that as a non-Newtonian viscous fluid. In von Boetticher et al. [57,58], the effective mixture viscosity is a complex linear combination between the phase viscosities, whereas in our formulation the mixture viscosities are complex and non-linear combinations between the solid and fluid-phase viscosities. The same applies for the velocities and pressures in our model while in the von Boetticher et al. [57] model the velocities and pressure are simply the bulk velocities and pressure.

10. Discussions and summary

The depth-averaged version of the two-phase mass flow model [18] has been successfully applied to different flows of mixture materials. Here, we focused on some particular aspects of the full-dimensional mixture flows down a channel. First, we considered the general three-dimensional and two-phase particle–fluid mixture mass flow model. Then, in order to develop a reduced but, generalized quasi two-phase bulk mixture model, we introduced the solid and fluid velocity drift coefficients, and also the pressure drift coefficient. From the application and computational point of view, this is useful, as it reduces the full two-phase model to quasi two-phase bulk model. This paves the way to apply the simple single-phase computational tools to numerically solve the new model equations. At the same time, the drifts contain important information relating the solid and fluid velocities, and the dynamic pressures. This makes the resulting model a generalized quasi two-phase bulk mixture model.

We developed two different mixture viscosities and pressures. The drift induced generalized mixture velocities are obtained. The effective bulk and shear viscosities are obtained by respectively averaging two alternative bulk and shear viscosities appearing in the model derivation. We noticed that the bulk and shear viscosities are identical. This can be considered as the mixture viscosity. The constructed mixture viscosity is rich in its physics and evolves mechanically as a coupled function of several physical and mechanical parameters and dynamical variables including the solid volume fraction, solid and fluid material densities and viscosities, solid friction and yield strength, rate of deformation of solid, and velocity and pressure drift parameters. This shows that the higher are the fluid drifts, faster is the fluid motion, and thus, higher is the deformation. This results in the lower bulk viscosity. In simple situations, the viscosity can be further reduced to the simplest description of the viscosity of the bulk mixture. We have also introduced a general concept of dynamically evolving drift induced generalized pressure for the bulk mixture flow. This shows that the pressure drift coefficient plays a crucial role in the pressure dynamics. We reveal that, during large shearing, dilatation and compaction, the mixture pressure may respond completely differently as compared to the solid or fluid pressure separately. Therefore, the dynamics of the bulk pressure is much more complex than just the dynamics of the solid and fluid pressures separately. For dilute flows, it reduces to the classical definition of the mixture pressure. The emergence of an effective mixture friction coefficient, that evolve dynamically, reveals one of the most important mechanical aspects of our mixture model. We have extended the pressure- and rate-dependent Coulomb-viscoplastic granular flow rheology to debris mixture flow. Such a sliding law for generalized bulk mixture dynamically defines the bottom boundary velocity.

With the constructed bulk mixture velocities and the pressure, the inertial coefficients, and the coefficients of dynamical mixture viscosities and pressure, our model for bulk mixture flow consists of the full two-dimensional quasi two-phase mass and momentum conservation equations. It appears that the dynamics of the bulk pressure, the inertial and dynamical coefficients are complex and coupled, and explicitly include the physics and dynamics of mixture. The final model equations are written as a well structured system of three non-linear partial differential equations in conservative form with three unknowns, namely, the generalized mixture velocities and pressure. This system is written in a convenient form for numerical simulations. Moreover, the newly derived mass and momentum equations appear in non-conventional form due to the inertial coefficients, and the non-equality of the mixture viscosities.

We outlined some important physical aspects, implications, and applicabilities of the new model. The model has a potential for a wider applications, it will be computationally faster than the full two-phase simulations, and, at the same time, more accurate than the single-phase models. The great advantages of the coupled and generalized model is that structurally it is the same as the existing single phase granular or debris flow model. So, in principle, the same computational strategy can be applied to solve this new system. However, the complexity and generality inherited by the two-phase bulk mixture flow are contained in the inertial, dynamical and pressure coefficients. Once mixture velocity and pressure are obtained, the two-phase dynamics of solid and fluid can be re-constructed from the definition of the mixture quantities and drift coefficients.

We derived reduced models as characterized either by the volume fraction, or by the drift coefficients. Solid volume fraction appears to be an internal variable for which an evolution equation can be constructed, or simply parameterized. In the most simplified situation, the model equations consist of a single velocity drift parameter. This is advantageous, because there are analytical expressions available for this. Alternatively, this factor can be obtained from the fast simulations of the depth averaged equations. This allows us to dynamically obtain the drift coefficient. For simple flow configuration with unit drift coefficients, the emerging model reduces to traditional effectively single-phase bulk mixture model. In special situation when the velocity and drifts are close to unity, the generalized mixture velocities, and pressure reduce to the classical barycentric velocities and pressure. This further reduces the complexity of the model system. For the identical velocity drift coefficients, the generalized viscosities reduce to a single classical mixture viscosity. In the most simple flow configuration, if further the velocity drifts are close to unity, then the mixture viscosity becomes the traditional simple bulk mixture viscosity. Even the simplest set of equations is important because this includes the first order basic dynamics of evolving mixture viscosity that governs the dynamics of the mixture flow.

Acknowledgements

We thank the reviewers, and the editor Giuseppe Saccomandi for their constructive reviews and suggestions that resulted in the substantially improved paper. We thank Albrecht von Boetticher for useful discussions on some mechanical aspects of the mixture flows. The idea of the model development and the model reduction was generated by Shiva P. Pudasaini. We gratefully acknowledge the financial support provided by the German Research Foundation (DFG) through the research project, PU 386/3-1: "Development of a GIS-based Open Source Simulation Tool for Modelling General Avalanche and Debris Flows over Natural Topography". Puskar R. Pokhrel acknowledges University Grants Commission (UGC), Nepal for the financial support provided as a Ph.D. fellowship (PhD-2071/072-Sci. & Tech. -01).

References

[1] A.M. Johnson, Physical Processes in Geology, Freeman, San Francisco, 1970.
[2] J.S. O'Brien, P.Y. Julien, W.T. Fullerton, Two-dimensional water flood and mud flow simulation, J. Hyd. Eng. 119 (2) (1993) 244–261.
[3] R.M. Iverson, R.P. Denlinger, Flow of variably fluidized granular masses across three-dimensional terrain: 1. Coulomb mixture theory, J. Geophys. Res. 106 (B1) (2001) 537–552.
[4] E.B. Pitman, L. Le, A two fluid model for avalanche and debris flows, Phil. Trans. R. Soc. A 363 (3) (2005) 1573–1601.

[5] S.P. Pudasaini, Y. Wang, K. Hutter, Modelling debris flows down general channels, Nat. Hazards Earth Syst. Sci. 5 (2005) 799–819.
[6] T. Takahashi, Debris Flow: Mechanics, Prediction and Countermeasures, Taylor and Francis, New York, 2007.
[7] E.B. Pitman, A.K. Patra, D. Kumar, K. Nishimura, J. Komori, Two phase simulations of glacial lake outburst flows, J. Comput. Sci. 4 (2013) 71–79.
[8] M. Mergili, J.-T. Fischer, J. Krenn, S.P. Pudasaini, r.avaflow v1, an advanced open source computational framework for the propagation and interaction of two-phase mass flows, Geosci. Model Dev. 10 (2017a) 553–569.
[9] R.M. Iverson, Elementary theory of bed-sediment entrainment by debris flows and avalanches, J. Geophys. Res. 117 (F03006) (2012) 197–200.
[10] M. Mergili, A. Emmer, A. Juricova, A. Cochachin, J.-T. Fischer, C. Huggel, S.P. Pudasaini, How well can we simulate complex hydro-geomorphic process chains? The 2012 multi-lake outburst flood in the Santa Cruz Valley (Cordillera Blanca, Peru), Earth Surf. Process. Landf. (2017c). http://dx.doi.org/10.1002/esp.4318.
[11] O. Hungr, S. McDougall, M. Bovis, A Real Two-Phase Submarine Debris Flow and Tsunami, Springer, Berlin, 2005.
[12] S.P. Pudasaini, J.-T. Fischer, A mechanical model for phase-separation in debris flow. 2016, arXiv:1610.03649v1.
[13] R.M. Iverson, The physics of debris flows, Rev. Geo-Phys. 35 (3) (1997) 245–296.
[14] S.P. Pudasaini, S.A. Miller, The hypermobility of huge landslides and avalanches, Eng. Geol. 157 (2013) 124–132.
[15] C.L. Chen, Generalized viscoplastic modelling of debris flow, J. Hydraul. Res. 114 (3) (1988) 237–258.
[16] P. Bohorquez, Study and Numerical Simulation of Sediment Transport in Free-Surface Flow (Ph.D. thesis), Málaga University, Málaga, 2008.
[17] E.D. Fernandez-Nieto, F. Bouchut, D. Bresch, M.J.C. Daz, A. Mangeney, A new Savage-Hutter type model for submarine avalanches and generated tsunami, J. Comput. Phys. 227 (16) (2008) 7720–7754.
[18] S.P. Pudasaini, A general two-phase debris flow model, J. Geophysics. Res. 117 (2012) F03010. http://dx.doi.org/10.1029/2011JF002186.
[19] S.P. Pudasaini, M. Krautblatter, A two-phase mechanical model for rock-ice avalanches, J. Geophys. Res. Earth Surf. 119 (2014). http://dx.doi.org/10.1002/2014JF003183.
[20] J. Kafle, P.R. Pokhrel, K.B. Khattri, P. Kattel, B.M. Tuladhar, S.P. Pudasaini, Submarine landslide and particle transport in mountain lakes, reservoirs and hydraulic plants, Ann. Glaciol. 57 (71) (2016) 232–244. http://dx.doi.org/10.3189/2016AoG71A034.
[21] P. Kattel, K.B. Khattri, P.R. Pokhrel, J. Kafle, B.M. Tuladhar, S.P. Pudasaini, Simulating Glacial lake outburst floods with a two-phase mass flow model, Ann. Glaciol. 57 (71) (2016) 349–358. http://dx.doi.org/10.3189/2016AoG71A039.
[22] M. Mergili, J.-T. Fischer, S.P. Pudasaini, Process chain modelling with r.avaflow: lessons learned from multi-hazard analysis. In: Advancing culture of living with landslides, WLF4, 2017b, 565–572.
[23] B. Domnik, S.P. Pudasaini, Full two-dimensional rapid chute flows of simple viscoplastic granular materials with a pressure-dependent dynamic slip-velocity and their numerical simulations, J. Non-Newton. Fluid Mech. 173–174 (2012) 72–86.
[24] B. Domnik, S.P. Pudasaini, R. Katzenbach, S.A. Miller, Coupling of full two-dimensional and depth-averaged models for granular flows, J. Non-Newton. Fluid Mech. 201 (2013) 56–68.
[25] C. Truesdell, Sulle basi della thermomeccanica, Rand Lincei, Series 8 (22) (1957) 33–38, 158–166.
[26] R.J. Atkin, R.E. Craine, Continuum theories of mixtures: Applications, J. Inst. Maths Appl. 17 (1976a) 153–207.
[27] R.J. Atkin, R.E. Craine, Continuum theories of mixtures: Basic theory and historical development, Quart. J. Mech. Appl. Math. 29 (1976b) 209–244.
[28] R.M. Bowen, in: A.C. Eringen (Ed.), Bowen RM Theory of Mixture, in: Continuum Physics, vol. 3, 1976, p. 1.
[29] A. Bedford, D.S. Drumheller, Recent advances: theories of immiscible and structured mixtures, Internat. J. Engrg. Sci. 21 (1983) 863–960.
[30] C. Truesdell, Rational Thermodynamics, Springer-Verlag, 1984.
[31] K.R. Rajagopal, L. Tao, Mechanics of Mixtures, vol. 754, World scientific, Singapore, 1995.
[32] M. Massoudi, Constitutive relations for the interaction force in multicomponent particulate flows, Int. J. Non-Linear Mech. 38 (2003) 313–336.
[33] M. Massoudi, A mixture theory formulation for hydraulic or pneumatic transport of solid particles, Int. J. Eng. Sci. 11 (2010) 1440–1461.
[34] S.B. Savage, K. Hutter, The motion of a finite mass of granular material down a rough incline, J. Fluid Mech. 199 (1989) 177–215.
[35] J.F. Richardson, W.N. Zaki, Sedimentation and fluidization: Part 1, Trans. Inst. Chem. Eng. 32 (1954) 35–53.
[36] M. Ishii, Thermo-Fluid Dynamic Theory of Two-Phase Flow, Eyrolles, Paris, 1975.
[37] M. Ishii, N. Zuber, Drag coefficient and relative velocity in bubbly, droplet or particulate flows, AIChE J. 25 (1979) 843–855.
[38] D.A. Drew, Mathematical modelling of two-phase flow, Ann. Rev. Fluid Mech. 15 (1983) 261–291.
[39] D.A. Drew, R.T. Lahey, The virtual mass and lift force on a sphere in rotating and straining inviscid flow, Int. J. Multiph. Flow. 13 (1987) 113–121.
[40] M. Rivero, J. Magnaudet, J. Fabre, Quelques resultants nouveaux concernat les forces exercees sur une inclusion spherique par unecoulement accelere, C. R. Acad. Sci. Ser. II 312 (1991) 1499–1506.
[41] R.M. Maxey, J.J. Riley, Equation of motion for a small sphere in a non-uniform flow, Phys. Fluids 26 (1993) 883–889.
[42] M. Ishii, T. Hibiki, Thermo-Fluid Dynamics of Two-Phase Flow, Springer, New York, 2006.
[43] N. Zuber, J. Findlay, Average volumetric concentration in two-phase flow systems, J. Heat Transf. 87 (1965) 453–468.
[44] G.B. Wallis, One-Dimensional Two-Phase Flow, McGraw-Hill, New York, 1969, p. 408.
[45] M. Manninen, V. Taivassalo, S. Kallio, On the Mixture Model for Multiphase Flow. Espoo, Technical Research Center of Finland, VTT Publications 228, ISBN: 951-38-4946-5, 1996 ISSN: 235-0621.
[46] B. Krasnopolsky, A. Starostin, A.A. Osiptsov, Unified graph-based multi-fluid model for gas-liquid pipeline flows, Comput. Math. Appl. 72 (2016) 1244–1262.
[47] M. Mills, Incompressible mixtures of newtonian fluids, Internat. J. Engrg. Sci. 4 (1966) 97–112.
[48] E. Bingham, Fluidity and Plasticity, McGrawHillZ, New York, 1922.
[49] P. Jop, Y. Forterre, O. Pouliquen, A constitutive law for dense granular flows, Coulomb mixture theory, Nature 441 (7094) (2006) 727–730.
[50] N.J. Balmforth, I. Frigaard, Viscoplastic fluids: From theory to application, J. Non-Newton. Fluid Mech. 142 (1–3) (2007) 1–3.
[51] Y. Forterre, O. Pouliquen, Flows of dense granular media, Annu. Rev. Fluid Mech. 40 (2008) 1–24.
[52] M. Pailha, O. Pouliquen, A two-phase flow description of the initiation of underwater granular avalanches, J. Fluid Mech. 633 (2009) 115–135.
[53] C. Ancey, Plasticity and geophysical flows, A review, J. Non-Newton. Fluid Mech. 142 (1–3) (2007) 4–35.
[54] J.D. Goddard, Dissipative materials as constitutive models for granular materials, Acta Mech. 63 (1996) 3–13.
[55] G.I. Tardos, A fluid mechanics approach to slow, frictional flow of powders, Powder Technol. 92 (1) (1997) 61–74.
[56] T. Schaefer, Viscosity spectral function of a scale invariant non-relativistic fluid from holography, Phys. Rev. 90 (2014) 106008.
[57] A. von Boetticher, J.M. Turowski, B.W. McArdell, D. Rickenmann, J.W. Kirchner, DebrisInterMixing-2.3: a finite volume solver for three-dimensional debris-flow simulations with two calibration parameters - Part 1: Model description, Geosci. Model Dev. 9 (2016) 2909–2923. http://dx.doi.org/10.5194/gmd-9-2909-2016.
[58] A. von Boetticher, J.M. Turowski, B.W. McArdell, D. Rickenmann, M. Hürlimann, DebrisInterMixing-2.3: a finite volume solver for three-dimensional debris - flow simulations with two calibration parameters - Part 2: Model validation, Geosci. Model Dev. 10 (2017) 3963–3978 http://dx.doi.org/10.5194/gmd-10-2017-25.
[59] S. Ghosh Hajra, S. Kandel, S.P. Pudasaini, Lie symmetry solutions for two-phase mass flows, Int. J. Non-Linear Mech. 77 (2015) 325–341.
[60] S.P. Pudasaini, Some exact solutions for debris and avalanche flows, Phys. Fluids 23 (4) (2011) 043301.
[61] S.P. Pudasaini, A novel description of fluid flow in porous and debris materials, Eng. Geol. 202 (2016) 62–73.
[62] K.K. Kuo, J.H. Koo, T.R. Davis, G.R. Coates, Transient combustion in mobile, gas-permeable propellants, Acta Astron. 3 (1976) 573–591.
[63] W. Prager, D.C. Drucker, Soil mechanics and plastic analysis or limit design, Q. Appl. Math. 10 (2) (1952) 157–165.
[64] S.P. Pudasaini, K. Hutter, S.-S. Hsiau, S.-C. Tai, Y. Wang, R. Katzenbach, Rapid flow of dry granular materials down inclined chutes impinging on rigid walls, Phys. Fluids 19 (5) (2007) 053302. http://dx.doi.org/10.1063/1.2726885.